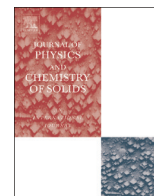




ELSEVIER

Contents lists available at ScienceDirect

## Journal of Physics and Chemistry of Solids

journal homepage: [www.elsevier.com/locate/jpcs](http://www.elsevier.com/locate/jpcs)

## Electron momentum density and Compton profile by a semi-empirical approach

Julio C. Aguiar<sup>a,\*</sup>, Darío Mitnik<sup>b,c</sup>, Héctor O. Di Rocco<sup>c,d</sup><sup>a</sup> Autoridad Regulatoria Nuclear, Av. Del Libertador 8250, C1429BNP Buenos Aires, Argentina<sup>b</sup> Instituto de Astronomía y Física del Espacio, and Facultad de Ciencias Exactas y Naturales, Universidad de Buenos Aires, C.C. 67, Suc. 28, C1428EGA Buenos Aires, Argentina<sup>c</sup> Consejo Nacional de Investigaciones Científicas y Técnicas (CONICET), Argentina<sup>d</sup> Instituto de Física "Arroyo Seco", CIFICEN (CONICET-UNCPBA), Pinto 399, 7000 Tandil, Argentina

## ARTICLE INFO

## Article history:

Received 8 December 2014

Received in revised form

25 March 2015

Accepted 26 March 2015

Available online 28 March 2015

## Keywords:

Compton profile

Electron momentum density

Local density

Approximation

Lam–Platzman correction

## ABSTRACT

Here we propose a semi-empirical approach to describe with good accuracy the electron momentum densities and Compton profiles for a wide range of pure crystalline metals. In the present approach, we use an experimental Compton profile to fit an analytical expression for the momentum densities of the valence electrons. This expression is similar to a Fermi–Dirac distribution function with two parameters, one of which coincides with the ground state kinetic energy of the free-electron gas and the other resembles the electron–electron interaction energy. In the proposed scheme conduction electrons are neither completely free nor completely bound to the atomic nucleus. This procedure allows us to include correlation effects.

We tested the approach for all metals with  $Z=3–50$  and showed the results for three representative elements: Li, Be and Al from high-resolution experiments.

© 2015 Elsevier Ltd. All rights reserved.

## 1. Introduction

Compton profile (CP) spectroscopy is a widely used tool to extract information about the electronic structure of crystalline solids. It provides the electron momentum density (EMD), which, in turn, allows the verification of the quality of the radial electron wave functions, since they are related through Fourier transforms. It is commonly accepted that many properties of the solids can be well represented by dividing the electrons into two groups: inner-core and conduction electrons. The former do not participate in crystalline bonding in solids and can be treated as frozen orbitals. Both bound and conduction electrons contribute to the total CP in different ways according to their spatial localization. Since conduction electrons are less bound, they have largely spread radial orbitals, and are therefore highly localized in momentum space. Thus, they contribute to the CP with a sharp peak located at low momentum transferred [1]. On the other hand, the electrons in the inner shells are strongly bound and have spatial orbits circumscribed to relatively small distances to the atomic nucleus. Their contribution to the CP takes place as a low-intensity broad tail at

high momentum transferred.

Historically, CPs obtained in experiments with high-resolution ( $\sim 0.1–0.2$  a.u.) X-ray have been successfully compared with those obtained by different theoretical methods, such as Quantum Monte Carlo [2,3], *ab initio* Green's function approximation [4], and DFT calculations with different exchange–correlation functionals [5–8]. The local density approximation (LDA) within the density functional theory (DFT) has been widely used to predict various bulk properties of different solids [9,10]. However, when theoretical CPs obtained by LDA calculations are compared with experimental ones, an overestimation at low momentum transfer and underestimation at high momentum transfer are observed. These discrepancies have been attributed to the incorrect exchange and correlation effects given by the LDA functional. Different methods based on Lam–Platzman correction [11–13] have been proposed to remedy the LDA deficiencies in the CP estimations. However, studies with high-resolution Compton scattering experiments of Li have revealed an anomalous behavior when it is compared with the theory [14–16], given that it has not been possible to describe by means of free-electron or by Fermi-liquid theory. Such deviations from the standard metallic picture can be ascribed to the possible existence of significant pairing correlations in the ground state identified in terms of electron transfers from s-like to p-like character, constituting a possible explanation for the breakdown of the Fermi-liquid picture [13,17].

\* Corresponding author. Fax: +54 11 6323 1375.

E-mail address: [jaguiar@arn.gob.ar](mailto:jaguiar@arn.gob.ar) (J.C. Aguiar).URL: <http://www.arn.gob.ar> (J.C. Aguiar).

For metallic systems one can define the Fermi surface (FS) as the break in the EMD whose presence reveals the existence of quasi-particles and the validity of the Landau–Fermi liquid theory. In this sense, the anti-symmetrized geminal product (AGP) method has been successfully used for a wide range of materials. This provides an orbital-dependent approach in which the electron momentum density is constructed using the natural orbitals, and the corresponding occupation numbers are obtained through a variational procedure [13,18].

In a recent work [19], high accuracy momentum densities and Compton profiles of Be, Cu, Ni, Fe<sub>3</sub>Pt, and YBa<sub>2</sub>Cu<sub>4</sub>O<sub>8</sub> were obtained using *ab initio* calculations of the linear tetrahedron method.

In this work, we propose a systematic approach to calculate the CPs of several crystalline metals by using a simple analytical expression for the valence EMD able to reproduce the CP with very high accuracy. The method allows including electron correlation effects based on the joint use of Fermi liquid and Hartree–Fock formalism. The formula proposed resembles the Fermi–Dirac distribution, but the thermodynamic constants are replaced by fitting parameters. A thorough and systematic investigation, led us to recognize that these fitting parameters are related to the Hartree–Fock energy of the free-electron ground state. These energies can be expressed either in terms of the Fermi momentum or, in terms of the Wigner–Seitz radius.

The present approach allows to calculate the CPs of all the metals with  $Z=3–50$ . Comparison with the experimental results showed good agreement in most of the cases. As an example, we show three selected metals with different valence values.

The rest of the paper is arranged as follows. Sections 2 and 3 describe the theoretical methods, especially the connections between kinetic and exchange energy of electrons in solids with thermodynamic distribution. Section 4 describes the comparison between our semi-empirical calculations and the experimental results for some representative elements. Finally, a brief summary is given in Section 5.

## 2. Theory

In a nonrelativistic and high-energy transfer regime, theoretical calculations for isotropic CPs are commonly performed under the impulse approximation (IA). It is assumed that energy and momentum are conserved. Limitations to the IA validity in Compton scattering have been widely discussed by [20]. This approach is expected to be valid when the energy transferred in the scattering process is much greater than the binding energy of the electron orbital.

The isotropic valence CP is defined under the IA as

$$J_{val}(q) = \frac{1}{2} \int_q^\infty n_{val}(p) p dp \quad (1)$$

being  $\int J_{val}(q) dq = N$ , where  $N$  is the number of valence electrons in the atom. Consequently, the valence EMD  $n_{val}(p)$ , can be obtained from the Compton profile by

$$n_{val}(p) = -\frac{2}{p} \frac{dJ_{val}}{dq} \Big|_{q=p}, \quad p \neq 0, \quad (2)$$

and

$$n_{val}(0) = -2 \frac{d^2 J_{val}}{dq^2}. \quad (3)$$

The free electron gas (FEG) CP is defined as

$$J^{FEG}(q) = \frac{1}{2} \int_q^\infty \frac{I_r(p)}{p} dp \quad (4)$$

where  $I_r(p)dp$  is the probability of an electron at position  $\mathbf{r}$  to have a momentum of magnitude between  $p$  and  $p + dp$ . The Thomas–Fermi theory states that, at zero temperature

$$I_r(p)dp = n_0 p^2 dp = \frac{4\pi}{(4/3)\pi k_F^3} p^2 dp, \quad (5)$$

where the Fermi momentum  $k_F$  is defined as

$$k_F = \frac{(9\pi/4)^{1/3}}{r_{WS}} \quad (6)$$

and  $r_{WS}$  is the Wigner–Seitz radius of a sphere containing a single electron [21]. Inserting  $Nn_0$  in place of  $n_{val}$  in Eq. (1), the FEG CP is

$$J^{FEG}(q) = \frac{3N}{4k_F^3} \left( k_F^2 - q^2 \right). \quad (7)$$

The CP given by Eq. (7) has the form of an inverted parabola for  $q \leq k_F$  and is zero for  $q > k_F$ . The same profile is produced by assuming a plane wave function  $e^{-i\mathbf{k}\cdot\mathbf{r}}/\sqrt{V}$  for the free electrons.

It should be noted that the valence EMD obtained from the non-interacting FEG CP (using Eq. (2)) coincides with the Fermi–Dirac distribution function:

$$f(p) = \left( 1 + \exp \left[ \frac{p^2/2 - \mu}{K_B T} \right] \right)^{-1} \quad (8)$$

where  $p^2/2$  is the energy of the single-particle state,  $\mu$  is the chemical potential ( $\sim k_F^2/2$ ), and  $K_B T$  is the thermal energy of the FEG [4]. Unfortunately, FEG model does not produce good results due to the effects of interactions with the periodic lattice potential and mutual electrons Coulomb interactions are neglected in these simple approaches.

## 3. Semiempirical approach

To generate parametric valence EMDs that lead to the correct CP values, we propose to use a modified Fermi–Dirac distribution function. As pointed out in [22], we can modify the Fermi–Dirac distribution with some broadening energy parameters. In our approach, we introduce  $\mu_e$  and  $T_e$ , called the *electronic chemical potential* and the *electronic Fermi temperature*, respectively, in analogy with the thermodynamic counterparts:

$$n_{val}(p) \equiv n_0 \left( 1 + \exp \left[ \frac{p^2/2 - \mu_e}{K_B T_e} \right] \right)^{-1}. \quad (9)$$

For a systematic study, we took the data from several CPs of pure crystalline metals ( $Z=3–50$ ) with the purpose to extract the valence EMD, as stated in Eq. (2). The elements and references used were: Li [14], Be [23], B [24], C (graphite) [25], Na [26,3], Mg [27], Al [28], Si [29], K [30], Ca [31], Sc [32], Ti [33], V [34], Cr [35], Mn [36], Fe [34], Co [37], Ni [34], Cu [38], Zn [39], Ga [40], Ge [29], Se [41], Rb [30], Sr [30], Y [42], Zr [43], Nb [30], Mo [44], Ru [45], Rh [46], Pd [47], Ag [48], Cd [39], In [30], and Sn [49].

To follow this approach, we rely on the fact that the derivative of the valence EMD  $\partial n_{val}(p)/\partial p$  provides information about the two required energies. This derivative function exhibits a peak at a momentum value corresponding to the electronic chemical potential  $\mu_e$ , and the spread of this function corresponds to the electronic Fermi energy  $k_B T_e$ . We must point out that these

energies are used only as an approximation tool, and are not the  $\mu$  and  $T$  from the truly Fermi–Dirac distribution. We must also emphasize that these energies should be different for each element.

Thus, we propose that these energies should coincide with the Hartree–Fock ground-state solution for free-electron plane waves [51,50]:

$$\frac{E}{N} = E_k - E_{exc} = \frac{3}{10}k_F^2 - \frac{3e^2k_F}{4\pi} \quad (10)$$

where the energies  $E_k$  and  $E_{exc}$  are the non-interacting kinetic and exchange energy, respectively. Two remarkable results raised from our research: First, the broadening energy  $K_B T_e$  adjusted notoriously with  $bE_k$ , where the parameter  $b$  is 1/4, 1/2 or 1 according to the Wigner–Seitz radius.

$$b = \begin{cases} 1/4 & 2 \leq r_{WS} < 2.4 \text{ and } 4 \leq r_{WS} < 5.75 \\ 1/2 & 1.8 \leq r_{WS} < 2 \text{ and } 2.4 \leq r_{WS} < 4 \\ 1 & 1 \leq r_{WS} < 1.8 \end{cases} \quad (11)$$

Moreover, the electronic chemical potential can be approximated with  $\mu_e = aE_{exc}$ , where  $a$  is 1 for monovalent metals including Mg, Ca and Sr, and 2 otherwise. If we associate this to the periodic table we can find some trends:  $b = 1/4$  for groups IA, IIIA and IVA, with exception of Li, B, and C, for which  $b = 1/2$ .  $b = 1/2$  for groups IIA, IB, IIB, IIIB, IVB, and part of VIII B (Co, Ni, Rh and Pd), and  $b = 1$  for groups VB, VIB, VIIB and part of VIII B (Fe, and Ru). The discrepant behavior of Li, B, and C can be ascribed to the possible existence of significant pairing correlations in the ground state identified in terms of electron transfers from s-like to p-like character, constituting a possible explanation for the breakdown of the Fermi-liquid picture [13,17].

Taking into account the mentioned striking resemblance between the fitting parameters and those energies, we propose a semi-empirical approach for the valence EMD, as

$$n_{val}^{SE}(p) = n_0 \left( 1 + \exp \left[ \frac{p^2/2 - aE_{exc}}{bE_k} \right] \right)^{-1} \quad (12)$$

Although this semi-empirical approach provides a good estimation of valence EMD, we can improve our results by including the effects of the atomic nucleus on the valence electrons. Hence, a more realistic calculation can be performed if we consider that conduction electrons are neither completely free nor completely bound to the atomic nucleus. In other words, the valence atomic electrons in a crystal lattice remain bound to the ion core while the distances to the nucleus are less than the Wigner–Seitz radius  $r_{WS}$ , and can be considered free for higher distances. Thus, we can include this effect in our approximation, by assuming that the atomic Hartree–Fock (HF) wave functions are valid solutions for small distances. Therefore, our final approximation formula for the valence EMD is

$$n_{val}^{app}(p) = \alpha \left[ n_{val}^{SE}(p) + \sum_{nl} \left| \chi_{nl}^{HFWS}(p) \right|^2 \right], \quad (13)$$

where  $\alpha$  is a normalization constant such as  $\int n_{val}^{app}(p) p^2 dp = N$ . The second term  $\chi_{nl}^{HFWS}(p)$  refers to the  $nl$  valence orbitals in the momentum space, obtained from the atomic Hartree–Fock radial wave functions  $R_{nl}(r)$  truncated at the Wigner–Seitz radius

$$\chi_{nl}^{HFWS}(p) = \left( \frac{2}{\pi} \right)^{1/2} (-i)^l \int_0^{r_{WS}} R_{nl}^{HF}(r) j_l(pr) r^2 dr, \quad (14)$$

being  $j_l(x)$  the spherical Bessel functions of the first kind. The CPs are obtained replacing the approximate valence EMD given by Eq. (13) in Eq. (1), which gives

$$J_{val}^{app}(q) = \beta \left[ J_{val}^{SE}(q) + \sum_{nl} J_{nl}^{HFWS}(q) \right], \quad (15)$$

where  $\beta$  is a normalization constant such as  $\int J_{val}^{app}(q) dq = N$ , and where the semi-empirical CP is obtained replacing Eq. (12) in Eq. (1)

$$J_{val}^{SE}(q) = \frac{3N}{20k_F^3} \left( 3bk_F^2 \ln \left[ \exp \left( \frac{5q^2}{3bk_F^2} \right) + \exp \left( \frac{5ae^2}{2\pi bk_F} \right) \right] - 5q^2 \right). \quad (16)$$

As stated in the previous section, the form of the free-electron density is a plateau with a parabolic border that is a sharp cliff producing a strong decrease in the corresponding CP. To connect smoothly the Fermi region to the HF (bound contribution), we weighed differently. For this purpose, we introduced a weight function  $W(q)$ , defined as

$$W^\pm(q) = \frac{1}{2} \left[ 1 \pm \tanh \left( \pi^2 \left( 1 - \frac{q}{k_F} \right) \right) \right]. \quad (17)$$

Then, as a further improvements of Eqs. (13) and (15), changing  $\sum_{nl} \left| \chi_{nl}^{HFWS}(p) \right|^2$  by  $n_{val}^{HFWS}(p)$ , and  $\sum_{nl} J_{nl}^{HFWS}(q)$  by  $J_{val}^{HFWS}(q)$  we propose our approximated valence EMD and CP formulas as

$$n_{val}^{app}(p) = W^+(p) n_{val}^{SE}(p) + W^-(p) n_{val}^{HFWS}(p), \quad (18)$$

and

$$J_{val}^{app}(q) = W^+(q) J_{val}^{SE}(q) + W^-(q) J_{val}^{HFWS}(q), \quad (19)$$

respectively.

## 4. Results

In Eq. (11) we have shown that the broadening parameter  $b$  can have values of 1/4, 1/2 or 1 according to Wigner–Seitz radius or the type of metal, i.e.  $b = 1/4$  for free-electron-like metals (Na, Al, Si, K, Ga, Ge, Rb and In). With respect to Al, Si, Ga, Ge and In ( $2 \leq r_{WS} < 2.4$ ) the Fermi region appears to be predominant and the Hartree–Fock contribution will be less than that for other elements, therefore a good approximation can be performed by making  $\frac{1}{2} n_{val}^{HFWS}(q)$  and  $\frac{1}{2} J_{val}^{HFWS}(q)$ . This anomalous behavior may be due to the fact that the electrons occupation number is largely described by the Fermi liquid region minimizing the contribution of bound electrons.

To demonstrate the applicability of our approach, the valence EMDs and the CPs were calculated using Eqs. (18) and (19), respectively, for three selected and representative metals. Comparisons with high-resolution (less than 0.15 a.u.) CPs values are presented for Li, Be and Al [14,23,28].

The atomic Hartree–Fock wave functions have been obtained by using the MCHF Fischer’s code [52]. Additionally and for comparisons, we show the results obtained by using the LDA calculations [53] with Lam–Platzman correction [11].

### 4.1. Lithium

Directional average CP in a cubic crystal may be reasonably obtained by [54]

$$J_{av}(q) = \frac{1}{35} \left[ 10J_{100}(q) + 16J_{110}(q) + 9J_{111}(q) \right]. \quad (20)$$

Results of the valence EMD for Li are presented in the left part of Fig. 1. The solid curve shows the EMD  $n_{val}^{app}(p)$  calculated using our semi-empirical approach (Eq. (18)). For comparisons, the CP experiment given by [14] was used to extract the EMD through Eq.

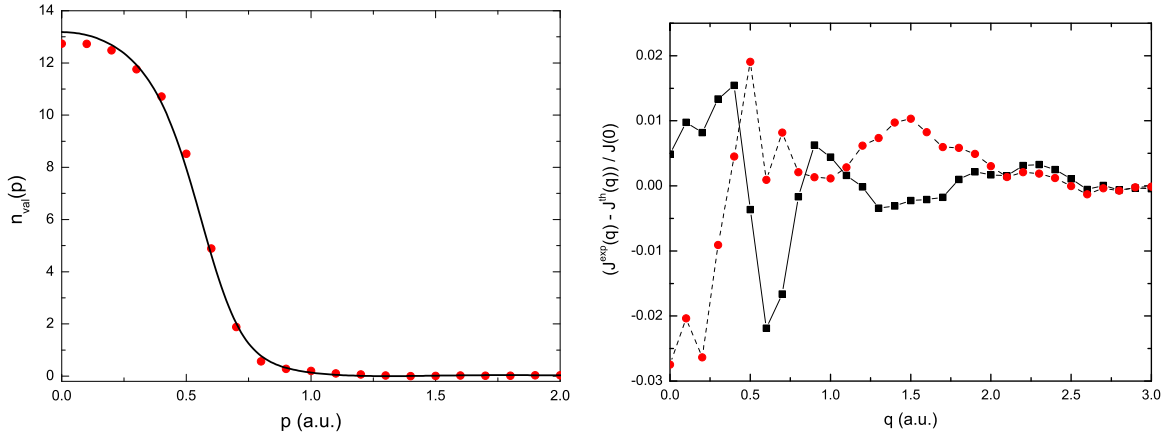


**Fig. 1.** Left: electron momentum density for Li, calculated with our semi-empirical approach (Eq. (18)) (black solid curve) and electron momentum density extracted from the Compton profile experiment reported by [14] (red circles). Right: differences between the experimental data and our semi-empirical approach (black squares solid). For comparison, the difference between experimental data and obtained data by local density approximation with Lam–Platzman correction is shown as red circles dashed. (For interpretation of the references to color in this figure caption, the reader is referred to the web version of this paper.)

(2). This experimental result is shown with the red circles in the same figure. The agreement between the EMD extracted from experiment and those obtained with our approximation formula is good for a wide range of momenta  $p$ .

The differences between the experimental and the theoretical values  $\Delta J_{val}(q) \equiv (J_{val}^{exp}(q) - J_{val}^{th}(q)) / J(0)$  as a function of the momentum transfer  $q$  are shown in the right part of Fig. 1. In this case, the differences are less than 2.2%. In addition, in the same figure we show the difference between the experiment and LDA calculation with Lam–Platzman correction. The LDA calculation was performed assuming a solid bulk as body centered cubic (*bcc*) of lattice constant 3.609 Å by minimizing the total energy; for comparison, the experimental lattice constant at room temperature is 3.5093 Å [55].

#### 4.2. Beryllium

Directional average CP in a hexagonal close packed (*hcp*) crystal structure was obtained by

$$J_{av}(q) = \frac{1}{7} [3J_{100}(q) + 3J_{110}(q) + J_{001}(q)]. \quad (21)$$

Result of the valence EMD for Be is presented in the left part of Fig. 2. Our semi-empirical approach is compared with the high-resolution CP experiment given by [23] as shown in the right part

of Fig. 2. An excellent agreement is obtained for a large range of momentum transfer. In this case, the differences are less than 1.5%. For comparison, in Fig. 2 we show the difference between the Compton profile experiment and LDA calculation with Lam–Platzman correction. For LDA calculations, we assumed an hexagonal close packed (*hcp*) crystal structure with lattice constants  $a=2.239$  Å and  $c=3.515$  Å by minimizing the total energy (the experimental lattice constants at room temperature are  $a=2.2859$  and  $c=3.5845$  Å [55]).

#### 4.3. Aluminium

Directional average CP in a face centered cubic (*fcc*) crystal was obtained by Eq. (20). Result of the valence EMD for Al as a function of the momentum is presented in the left part of Fig. 3. Our approach is compared with the high-resolution experimental data given by [28]. An excellent agreement is obtained for a large range of momentum transfer. In this case, the differences are less than 2%. For comparison, in Fig. 3 we show the difference between the Compton profile experiment and LDA calculation with Lam–Platzman correction. The LDA calculation was performed assuming a face centered cubic (*fcc*) packed crystal structure with lattice constant  $a=3.969$  Å by minimizing the total energy (the experimental lattice constant at room temperature is  $a=4.04958$  Å [55]).

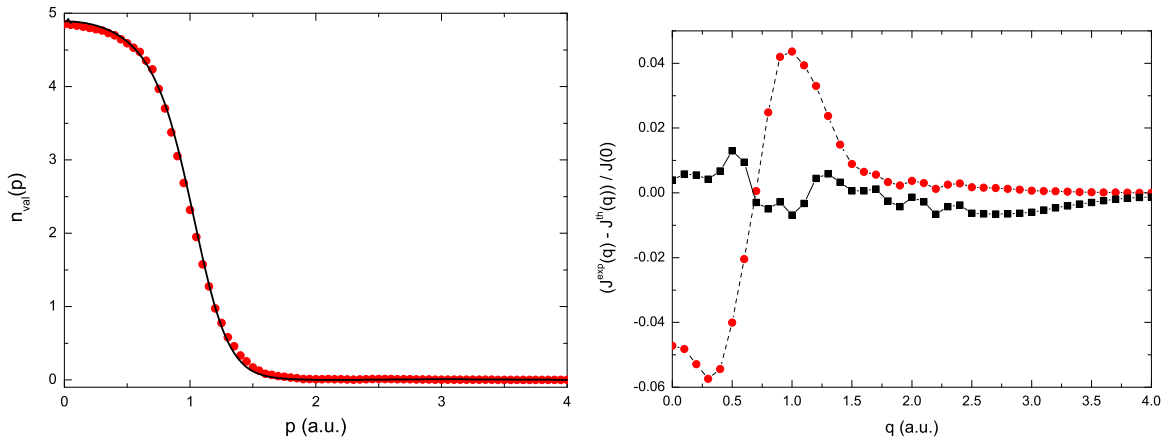


**Fig. 2.** Left: electron momentum density for Be, calculated with our semi-empirical approach (Eq. (18)) (black solid curve) and extracted from experimental data reported by [23] (red circles). Right: differences between the experimental data and our theory (black squares solid). For comparison, the difference between experimental data and obtained data by local density approximation with Lam–Platzman correction is shown as red circles dashed. (For interpretation of the references to color in this figure caption, the reader is referred to the web version of this paper.)

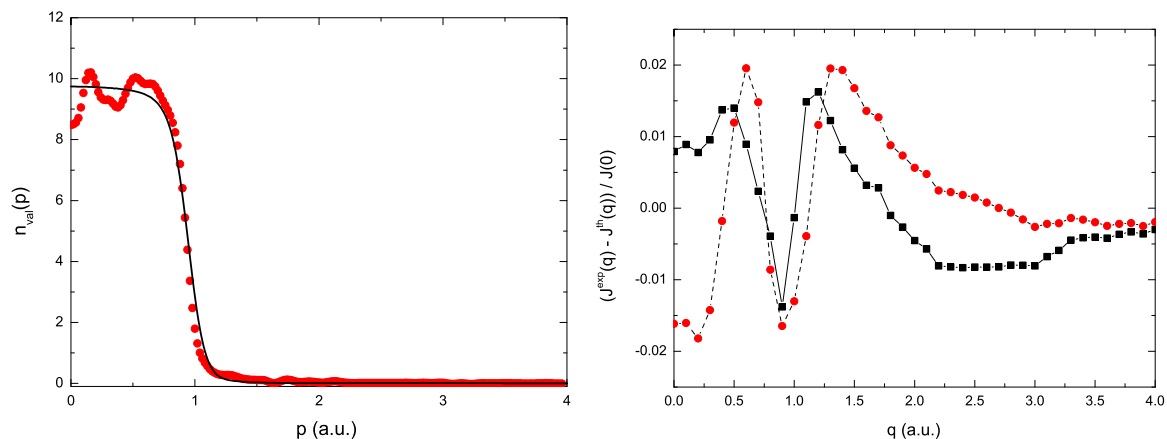


**Fig. 3.** Left: electron momentum density of Al, calculated with our semi-empirical approach (Eq. (18)) (black solid curve) and extracted from the Compton profile result reported by [28] (red circles). Right: differences between the experimental data and our semi-empirical approach (black squares solid). For comparison, the difference between experimental data and obtained data by local density approximation with Lam–Platzman correction is shown as red circles dashed. (For interpretation of the references to color in this figure caption, the reader is referred to the web version of this paper.)

## 5. Conclusions

Based on a modified Fermi–Dirac distribution function and Hartree–Fock formalism, we demonstrated that Fermi break is of the same order as exchange energy at an effective temperature. Similar behaviors have been suggested by [13,17,18]. Therefore, the present semi-empirical method captures pairing correlation effects in the same way as the anti-symmetrized geminal product theory. Furthermore, it reveals important correlation effects beyond the Landau–Fermi liquid picture.

Clearly, our general approach is in excellent agreement when is compared with high-resolution Compton profile experiments, or with LDA approximation plus Lam–Platzman correction.

On the other hand, valence Compton profiles using the scheme presented here might be very useful e.g. for data reduction of inelastic x-ray scattering from bound electrons (x-ray Raman scattering), in which absorption edge-like features can be superimposed by strong contribution of the valence electron Compton profile [56–58]. Here valence Compton profiles can be used for background subtraction. In addition, our method could explain some anomalies observed in  $\text{Al}_{97}\text{Li}_3$  alloys [59].

We compared the results of our approach with results from other materials, such as LiF, NaCl, MgO, and BeO, and found good agreement in most cases using the parameters  $a=2$  and  $1/2 \leq b < 3/2$ , however, these last issues are under investigation.

## Acknowledgments

We thank the support from Universidad Nacional del Centro de la Provincia de Buenos Aires (UNCPBA, Argentina). We also thank G. Stutz, S. Huotari and Y. Sakurai for kindly providing us with the high resolution Compton profiles of lithium, beryllium and aluminium, respectively. D.M. acknowledges support by UBACyT 239 from Universidad de Buenos Aires, and PIP 200901/552 from CONICET Argentina.

## References

- [1] M.J. Cooper, P.E. Mijnarends, N. Shiotani, N. Sakai, A. Bansil (Eds.), *X-Ray Compton Scattering*, Oxford University Press, New York, 2004.
- [2] M. Holzmann, B. Bernu, C. Pierleoni, J. McMinis, D.M. Ceperley, V. Olevano, L. Delle Site, *Phys. Rev. Lett.* 107 (2011) 110402.
- [3] S. Huotari, J.A. Soininen, T. Pylkkänen, K. Hämäläinen, A. Issolah, A. Titov, J. McMinis, J. Kim, K. Esler, D.M. Ceperley, M. Holzmann, V. Olevano, *Phys. Rev. Lett.* 105 (2010) 086403.

- [4] V. Olevano, A. Titov, M. Ladisa, K. Hämäläinen, S. Huotari, M. Holzmann, *Phys. Rev. B* 86 (2012) 195123.
- [5] A. Erba, C. Pisani, S. Casassa, L. Maschio, M. Schütz, D. Usvyat, *Phys. Rev. B* 81 (2010) 165108.
- [6] C. Pisani, A. Erba, S. Casassa, M. Itou, Y. Sakurai, *Phys. Rev. B* 84 (2011) 245102.
- [7] C. Pisani, M. Itou, Y. Sakurai, R. Yamaki, M. Ito, A. Erba, L. Maschio, *Phys. Chem. Chem. Phys.* 13 (2011) 933.
- [8] A. Erba, M. Itou, Y. Sakurai, R. Yamaki, M. Ito, M. Casassa, L. Maschio, A. Terentjev, C. Pisani, *Phys. Rev. B* 83 (2011) 125208.
- [9] R.O. Jones, O. Gunnarsson, *Rev. Mod. Phys.* 61 (1989) 689.
- [10] V.L. Moruzzi, J.F. Janak, A.R. Williams, *Calculated Electronic Properties of Metals*, Pergamon Press Inc., New York, 1978.
- [11] L. Lam, P. Platzman, *Phys. Rev. B* 9 (1974) 5122.
- [12] D.A. Cardwell, M.J. Cooper, *J. Phys.: Condens. Matter* 1 (1989) 9357.
- [13] B. Barbiellini, A. Bansil, *J. Phys. Chem. Solids* 62 (2001) 2181.
- [14] W. Schülke, G. Stutz, F. Wohler, A. Kaprolat, *Phys. Rev. B* 54 (1996) 14381.
- [15] C. Sternemann, T. Buslaps, A. Shukla, P. Suortti, G. Döring, W. Schülke, *Phys. Rev. B* 63 (2001) 094301.
- [16] H. Bross, *Phys. Rev. B* 72 (2005) 115109.
- [17] D. Nissenbaum, L. Spanu, C. Attacalite, B. Barbiellini, A. Bansil, *Phys. Rev. B* 79 (2009) 035416.
- [18] B. Barbiellini, *Low Temp. Phys.* 40 (2014) 318.
- [19] D. Ernstring, D. Billington, T.D. Haynes, T.E. Millichamp, J.W. Taylor, J.A. Duffy, S. R. Giblin, J.K. Dewhurst, S.B. Dugdale, *J. Phys.: Condens. Matter* 26 (2014) 495501.
- [20] I.G. Kaplan, B. Barbiellini, A. Bansil, *Phys. Rev. B* 68 (2003) 235104.
- [21] S. Lundqvist, N.H. March, *Theory of the Inhomogeneous Electron Gas*, Plenum Press, New York, 1983.
- [22] J. Kohanoff, *Electronic Structure Calculations for Solids and Molecules: Theory and Computational Methods*, Cambridge University Press, New York, 2006, p. 137.
- [23] S. Huotari, K. Hämäläinen, S. Manninen, S. Kaprzyk, A. Bansil, W. Caliebe, T. Buslaps, V. Honkimäki, P. Suortti, *Phys. Rev. B* 62 (2000) 7956.
- [24] R.J. Weiss, *Philos. Mag.* 21 (1970) 1169.
- [25] J. Felsteiner, I. Gertner, *J. Appl. Phys.* 52 (1981) 1592.
- [26] P. Eisenberger, L. Lam, P.M. Platzman, P. Schmidt, *Phys. Rev. B* 6 (1972) 3671.
- [27] P. Rennert, G. Carl, U.H. Gläser, *Phys. Status Solidi B* 115 (1983) 219.
- [28] T. Ohata, M. Itou, I. Matsumoto, Y. Sakurai, H. Kawata, N. Shiotani, S. Kaprzyk, P. E. Mijnarends, A. Bansil, *Phys. Rev. B* 62 (2000) 16528.
- [29] W.A. Reed, P. Eisenberger, *Phys. Rev. B* 6 (1972) 4596.
- [30] N.I. Papanicolaou, N.C. Bacalis, D.A. Papaconstantopoulos, *Handbook of Calculated Electron Momentum Distribution, Compton profiles, and X-Ray Form Factors of Elemental Solids*, CRC Press, Florida, 1991.
- [31] S.K. Danakas, K.T. Kotsis, N.I. Papanicolaou, *Phys. Status Solidi B* 209 (1998) 81.
- [32] T. Paakkari, K.-F. Berggren, R. Ribberfors, V. Halonen, *Phys. Rev. B* 14 (1976) 2301.
- [33] J.C. Aguiar, H.O. Di Rocco, D. Mitnik, *J. Phys. Chem. Solids* 74 (2013) 1341.
- [34] T. Paakkari, S. Manninen, K.-F. Berggren, *Phys. Fenn.* 10 (1975) 207.
- [35] S. Wakoh, Y. Kubo, J. Yamashita, *J. Phys. Soc. Jpn.* 40 (1976) 1043.
- [36] A. Gupta, B.K. Sharma, B.L. Ahuja, *Pramana—J. Phys.* 31 (1988) 225.
- [37] B.L. Ahuja, B.K. Sharma, O. Aikala, *Pramana—J. Phys.* 29 (1987) 313.
- [38] Y. Sakurai, S. Kaprzyk, A. Bansil, Y. Tanaka, G. Stutz, H. Kawata, N. Shiotani, *J. Phys. Chem. Solids* 60 (1999) 905.
- [39] S. Perkkio, B.K. Sharma, S. Manninen, T. Paakkari, B.L. Ahuja, *Phys. Status Solidi B* 168 (1991) 657.
- [40] B. Lengeler, R. Lasser, G. Mair, *Phys. Rev. B* 22 (1980) 5748.
- [41] U. Bonse, W. Schröder, W. Schülke, *Solid State Commun.* 21 (1977) 807.
- [42] B.L. Ahuja, M.D. Sharma, B.K. Sharma, S. Hamouda, M.J. Cooper, *Phys. Scr.* 50

- (2006) 301.
- [43] B.K. Sharma, B.L. Ahuja, Phys. Rev. B 38 (1988) 3148.
- [44] B.K. Sharma, B.L. Ahuja, H. Singh, F.M. Mohammad, Pramana—J. Phys. 40 (1993) 399.
- [45] R.K. Kothari, K.B. Joshi, M.D. Sharma, B.L. Ahuja, B.K. Sharma, Phys. Status Solidi B 190 (1995) 475.
- [46] B.L. Ahuja, V. Sharma, A. Rathor, A.R. Jani, B.K. Sharma, Nucl. Instrum. Methods Phys. Res. 262 (2007) 391.
- [47] B.K. Sharma, A. Gupta, H. Singh, S. Perkkio, A. Kshirsagar, D.G. Kanhere, Phys. Rev. B 37 (1988) 6821.
- [48] A. Andrejczuk, L. Dobrzynski, J. Kwiatkowska, F. Maniawski, S. Kaprzyk, A. Bansil, E. Zukowski, M.J. Cooper, Phys. Rev. B 48 (1993) 15552.
- [49] B.L. Ahuja, S. Khera, S. Mathur, N.L. Heda, Phys. Status Solidi B 243 (2006) 625.
- [50] N.W. Ashcroft, N.D. Mermin, Solid State Physics, Brooks Cole, Pacific Grove, CA, 1976, p. 336.
- [51] J.C. Slater, Phys. Rev. 81 (1951) 385.
- [52] C.F. Fischer, Comput. Phys. Commun. 64 (1991) 369.
- [53] (<http://www.openmx-square.org/>).
- [54] M. Miasek, J. Math. Phys. 7 (1966) 139.
- [55] H.W. King, CRC Handbook of Chemistry and Physics, vol. 83, 2002, p. 19.
- [56] T.T. Fister, K.P. Nagle, F.D. Vila, G.T. Seidler, C. Hamner, J.O. Cross, J.J. Rehr, Phys. Rev. B 79 (2009) 174117.
- [57] H. Sternemann, C. Sternemann, G.T. Seidler, T.T. Fister, A. Sakko, M. Tolan, J. Synchrotron Radiat. 15 (2008) 162.
- [58] Ch.J. Sahle, A. Mirone, J. Niskanen, J. Inkinen, M. Krisch, S. Huotari, J. Synchrotron Radiat. 22 (2015) 400.
- [59] J. Kwiatkowska, B. Barbiellini, S. Kaprzyk, A. Bansil, H. Kawata, N. Shiotani, Phys. Rev. Lett. 96 (2006) 186403.